

## Research Paper

# $\beta$ -glucan-coupled superparamagnetic iron oxide nanoparticles induce trained immunity to protect mice against sepsis

Yuchen Pan<sup>1</sup>, Jingman Li<sup>1</sup>, Xiaoyu Xia<sup>1</sup>, Jiali Wang<sup>1</sup>, Qi Jiang<sup>1</sup>, Jingjing Yang<sup>1</sup>, Huan Dou<sup>1</sup>, Huaping Liang<sup>2</sup>✉, Kuanyu Li<sup>1</sup>✉ and Yayi Hou<sup>1,3</sup>✉

1. State Key Laboratory of Pharmaceutical Biotechnology, Division of Immunology, Medical School, Nanjing University, Nanjing 210093, China.
2. State Key Laboratory of Trauma, Burns and Combined Injury, Research Institute of Surgery, Daping Hospital, The Army Medical University, Chongqing 400042, China.
3. Jiangsu Key Laboratory of Molecular Medicine, Nanjing 210093, China.

✉ Corresponding authors: Yayi Hou, E-mail: yayihou@nju.edu.cn; Kuanyu Li, E-mail: likuanyu@nju.edu.cn; Huaping Liang, E-mail: 13638356728@163.com.

© The author(s). This is an open access article distributed under the terms of the Creative Commons Attribution License (<https://creativecommons.org/licenses/by/4.0/>). See <http://ivyspring.com/terms> for full terms and conditions.

Received: 2021.07.12; Accepted: 2021.11.12; Published: 2022.01.01

## Abstract

**Background:** Innate immune memory, also termed “trained immunity”, is thought to protect against experimental models of infection, including sepsis. Trained immunity via reprogramming monocytes/macrophages has been reported to result in enhanced inflammatory status and antimicrobial activity against infection in sepsis. However, a safe and efficient way to induce trained immunity remains unclear.

**Methods:**  $\beta$ -glucan is a prototypical agonist for inducing trained immunity. Ferumoxytol, superparamagnetic iron oxide (SPIO) with low cytotoxicity, has been approved by FDA for clinical use. We synthesized novel nanoparticles BSNPs by coupling  $\beta$ -glucan with SPIO. BSNPs were further conjugated with fluorescein for quantitative analysis and trace detection of  $\beta$ -glucan on BSNPs. Inflammatory cytokine levels were measured by ELISA and qRT-PCR, and the phagocytosis of macrophages was detected by flow cytometry and confocal microscopy. The therapeutic effect of BSNPs was evaluated on the well-established sepsis mouse model induced by both clinical *Escherichia coli* (*E. coli*) and cecal ligation and puncture (CLP).

**Results:** BSNPs were synthesized successfully with a 3:20 mass ratio of  $\beta$ -glucan and SPIO on BSNPs, which were mainly internalized by macrophages and accumulated in the lungs and livers of mice. BSNPs effectively reprogrammed macrophages to enhance the production of trained immunity markers and phagocytosis toward bacteria. BSNP-induced trained immunity protected mice against sepsis caused by *E. coli* and CLP and also against secondary infection. We found that BSNP treatment elevated Akt, S6, and 4EBP phosphorylation, while mTOR inhibitors decreased the trained immunity markers and phagocytosis enhanced by BSNPs. Furthermore, the PCR Array analysis revealed *Igf1*, *Sesn1*, *Vegfa*, and *Rps6ka5* as possible key regulators of mTOR signaling during trained immunity. BSNP-induced trained immunity mainly regulated cellular signal transduction, protein modification, and cell cycle by modulating ATP binding and the kinase activity. Our results indicated that BSNPs induced trained immunity in an mTOR-dependent manner.

**Conclusion:** Our data highlight that the trained immunity of macrophages is an effective strategy against sepsis and suggest that BSNPs are a powerful tool for inducing trained immunity to prevent and treat sepsis and secondary infections.

Key words: Sepsis; Macrophages; Trained immunity;  $\beta$ -glucan; SPIO

## Introduction

Sepsis is a major socioeconomic burden worldwide [1-3] and defined as a clinical syndrome characterized by multiple organ failure due to dysregulated host response to infection [4-6]. Despite rapid advances in early diagnosis and the use of

antibiotics and personalized treatment, sepsis still has a mortality rate of up to 25% [7-8]. Moreover, coronavirus disease 2019 (COVID-19) could be better described as “viral sepsis” [9-10], since some patients with COVID-19 met the diagnostic criteria for septic

shock and sepsis [11-12]. Therefore, we focused on developing preventive measures or broad-spectrum therapy for sepsis.

Innate immune response boosted after experiencing initial stimulus, termed as “trained immunity”, is a powerful defense against infection, regardless of bacteria, fungi or virus [13].  $\beta$ -glucan-mediated trained immunity in cells induced the epigenetic reprogramming of myeloid cells, especially monocytes and macrophages [14], resulting in an enhanced inflammatory status [15] and antimicrobial activity [16]. Trained immunity also protected dogs against rabies [17] and mice against a lethal dose of *Candida albicans* [18] and *Mycobacterium tuberculosis* [19]. As trained immunity can lead to nonspecific protection from re-infection, it may provide a new tool for preventing and treating sepsis [20]. Thus, it is essential to explore secure and efficient ways to induce trained immunity.

The emergence of nanotechnology offers an opportunity to use nanoparticles as carriers for vaccine and drug delivery [21-23]. Ferumoxytol, superparamagnetic iron oxide (SPIO) with low cytotoxicity, has been approved by FDA for clinical use as an iron supplement [24-25]. After coupling with other materials, SPIO could be used for the diagnosis and treatment of lung [26], liver [27-28], and colon cancers [29]. Disruption of iron homeostasis is a common feature of sepsis, characterized by decreased serum iron and transferrin levels [30-31]. Lactoferrin supplementation reduced late-onset sepsis in preterm infants without adverse effects [32]. Our previous studies showed that SPIO alleviated LPS-induced sepsis in mice by promoting macrophages to secrete IL-10 [33]. However, it was still unclear whether proper engineering of SPIO with  $\beta$ -glucan could efficiently induce the trained immunity of macrophages against infection in sepsis.

In the current study, we synthesized  $\beta$ -glucan-coupled SPIO nanoparticles (BSNPs) and investigated their protective effect in the clinical *E. coli*- and CLP-induced sepsis mouse model. We found that BSNP-induced trained immunity improved macrophage phagocytosis of bacteria and promoted macrophages to produce inflammatory factors to kill bacteria in an mTOR-dependent manner. Importantly, BSNP treatment could prevent sepsis and also protect mice against secondary infection. Our data indicated BSNPs as a potential strategy for sepsis prevention and treatment by promoting trained immunity.

## Materials and methods

### Reagents

LPS (*E. coli* O55:B5) and  $\beta$ -glucan (CAS: 9041-22-9) were purchased from Sigma (Shanghai, China)

and prepared in double distilled water (ddH<sub>2</sub>O). M-CSF (Novoprotein, Shanghai, China) for BMDM was prepared in ddH<sub>2</sub>O. Rapamycin (HY-10219), Torkinib (HY-10474) and WAY600 (HY-15272) were purchased from MedChemExpress (MCE, Monmouth Junction, NJ, USA) and prepared in DMSO. The antibodies used for flow cytometry (supplemental Table S1) and PCR Assay plates (Wcgene Biotech, Shanghai, China) were all purchased from fcmacs (Nanjing, China). Superparamagnetic iron oxide nanoparticles (SPIO, Ferumoxytol) was kindly provided by professor Ning Gu from Southeast University.

### Cells and Culture Conditions

Raw264.7 cells and mice peritoneal macrophages were cultured in DMEM (Gibco, Grand Island, NY, USA) containing 10% FBS (Gibco), 1% penicillin and streptomycin (100  $\mu$ g/mL; Gibco BRL, USA), at 37 °C in a humidified atmosphere with 5% CO<sub>2</sub>.

### Bacterial Strain

The clinical strains of *E. coli* (*E. coli*<sup>a</sup> for short) were isolated from human clinical specimens, and identified by the Medical Laboratory Center of Zhongda Hospital in Nanjing, Jiangsu, China. Bacterial strains were stored at -80 °C and prepared in LB Medium or LB-Agar medium before use.

### Mice

Female ICR mice at 6-8 weeks old were obtained from Sino-British SIPPR/BK Lab. Animal Ltd (Shanghai, China). They were acclimatized for 5-7 days before molding. All procedures involving animals were in strict accordance with protocols that approved by the Research Ethics Committee of Nanjing University. Mice were housed in specific pathogen-free conditions at the Nanjing University Animal Care Commission. At the end of the experiment, mice were terminated humanely.

### Experimental sepsis

Early removal criteria: 1) Weight loss: loss of 20% of their baseline body weight; 2) Weakness/ inability to obtain feed or water: inability or extreme reluctance to stand/ambulate for 24 hours.

*E. coli*<sup>a</sup> grown to mid-exponential phase was harvested, washed and resuspended with normal saline. Mice were injected intraperitoneally (i.p.) with 0.2 mL bacterial suspension. Mortality was recorded after mice injected with lethal dose of *E. coli*<sup>a</sup>.

Polymicrobial sepsis was induced by cecal ligation and puncture (CLP). Briefly, after anesthesia with pentobarbital, mice were placed on electric homeothermic blanket to maintain body temperature at 36.5 °C. The cecum was ligated below the ileocecal

valve through a small abdominal incision and subjected to a single “through-and-through” perforation (20-gauge needle). Then the abdominal incision was closed in layers. Mice in sham group underwent the same surgical without ligation and puncture on cecum. Body weight was recorded every day before sacrifice.

### Trained immunity *in vivo*

Mice were injected intraperitoneally with normal saline (group c),  $\beta$ -glucan (500  $\mu$ g, group b), SPIO (150  $\mu$ g, group s),  $\beta$ -glucan (500  $\mu$ g) combined with SPIO (150  $\mu$ g) (group bs) or BSNPs (SPIO 150  $\mu$ g composited with  $\beta$ -glucan 22.5  $\mu$ g, group n) twice a week before sacrifice or *E. coli*<sup>a</sup> injection. Mice from each group injected with *E. coli*<sup>a</sup> were marked as c-E, b-E, s-E, bs-E or n-E.

### Trained immunity *in vitro*

Mice macrophage cell line Raw264.7 cells were treated for 24 h with  $\beta$ -glucan (30  $\mu$ g/mL, group b), SPIO (200  $\mu$ g/mL, group s),  $\beta$ -glucan (30  $\mu$ g/mL) combined with SPIO (200  $\mu$ g/mL) (group bs) or BSNP (SPIO 200  $\mu$ g composited with  $\beta$ -glucan 30  $\mu$ g/mL, group n). Then cells were washed with PBS for 3 times, and cultured with fresh medium for 5 days before use.

### Histology and Tissue Injury Scoring

Lung and liver tissue sections were stained with hematoxylin and eosin (H&E) and observed under a light microscope. Based on the presence of exudates, hyperemia/congestion, infiltration of inflammatory cells, morphological changes of lung tissue were scored as nil (0), mild (+1), moderate (+2), or severe (+3) injury [34–35]. Based on the vacuolization, sinusoidal congestion, and hepatocyte necrosis, liver injuries were scored from 0 to 4 [36]. The sum of scores of different animals was averaged.

### Synthesis of BSNPs

Superparamagnetic iron oxide nanoparticles (SPIO; 20 mg, containing carboxyl groups on the surface) were first dissolved in a solution of 20 mL ddH<sub>2</sub>O containing 1-ethyl-3-(3-dimethylamino-propyl) carbodiimide hydrochloride (EDC; 22 mg) (Bidepharm, Shanghai, China). The mixture was then stirred at room temperature for 30 min and  $\beta$ -glucan (4 mg) was then added to the mixture and stirred overnight at room temperature. Thereafter, the reaction mixture was concentrated and then added excess ethanol to obtain crude BSNPs. The crude products were resuspended with ddH<sub>2</sub>O, washed with excess ethanol, and then dried under reduced pressure.

### Synthesis of BSNP-RhB or BSNP-NIR

First,  $\beta$ -glucan (10 mg) and Rhodamine B isothiocyanate (RhB; 0.5 mg; CAS: 36877-69-7) or NIR-797 (NIR; 0.5 mg; CAS: 152111-91-6) were added into a 10 mL flask with 5 mL dimethyl sulfoxide (DMSO; Sigma). The mixture was stirred overnight at room temperature, and then diluted with 20 mL deionized water. The diluted mixture was dialyzed against 2 L of ddH<sub>2</sub>O in a 3.5 kDa MWCO for two days to remove the unreacted RhB or NIR. The products were dried under reduced pressure to obtain fluorescence-glucan and used to synthesize fluorescence-BSNPs (BSNP-RhB or BSNP-NIR) with the same protocol as BSNPs.

### Quantitative Analysis of $\beta$ -glucan on BSNPs

BG-RhB was diluted with ethanol to perform five two-fold serial dilutions in separate tubes. After diluting, the BG-RhB concentrations are 0.4 mg/mL, 0.2 mg/mL, 0.1 mg/mL, 0.05 mg/mL and 0.025 mg/mL, respectively. Ethanol serves as the zero standard (0 mg/mL). Full-function Fluorescence Spectrometer (FLS920, Edinburgh Instruments, UK) was used to detect the spectrum, create fit curve and calculate integration area. Plot the standard curve with concentration on the x-axis and integration area on the y-axis to create standard formula (Supplemental Table S2). During synthesis BSNP-RhB, a certain volume of washing ethanol was collected. The washing ethanol was then diluted with ethanol to perform different samples to make it more accurate. Spectrum and integration area of samples were detected with fluorescence spectrometer. The standard formula was used to calculate the concentration of each sample.

The theoretical density of molecules on nanoparticle surface  $\rho$  can be calculated via:

$$\rho = \frac{m}{MNS}$$

where the mass of  $\beta$ -glucan  $m$  can be calculated via standard formula, the average molecular weight of glucan  $M$  that we used was about 30,000, the number of nanoparticles  $N$  can be determined by Dynamic Light Scattering, and the superficial area of nanoparticles  $S$  can be calculated with average diameter that determined by Transmission Electron Microscopy (TEM). The theoretical density of glucan on BSNPs surface is 0.005 mol/m<sup>2</sup>, and molecules of glucan on BSNPs surface is around 3000 /nm<sup>2</sup>.

### Bio-distribution analysis of BSNPs

BSNP-NIR was intraperitoneally injected into mice. After 24 h, the *ex vivo* imaging of major organs was performed using *In vivo* Imaging System (LB 983 NC100, Berthold, Germany). BSNP-RhB was

intraperitoneally injected into mice, and peritoneal macrophage was washed with PBS for two times to obtain single cell suspension for fluorescent antibody staining. BSNPs uptake by macrophages were measured by confocal microscope or flow cytometry.

### Enzyme Linked Immunosorbent Assay (ELISA)

TNF $\alpha$ , IL-1 $\beta$  and IL-6 were measured using ELISA kit according to the manufacturer protocol (TNF $\alpha$  and IL-6: BioLegend; IL-1 $\beta$ : R&D). Cells were lysed with ddH<sub>2</sub>O. Supernatants and lysates were collected and stored at -80 °C until assayed.

### Western Blot

Proteins were exacted with RIPA lysis buffer (Beyotime, Shanghai, China) as protocol described. After electrophoresis on SDS-PAGE, proteins were transferred onto PVDF membranes (Millipore). The antibodies used for western blot and immunofluorescence were all purchased from Cell Signaling Technologies (CST, Beverly, MA, USA; Supplemental Table S3).

### Immunofluorescence

For immunofluorescence analysis, cells were seed on the plates pre-coated with cover slides. At the end of experiment, 4% paraformaldehyde (PFA) was added onto each pore for 10 min, and then wash cells with ddH<sub>2</sub>O at least 3 times. The cover slides were then placed on the glass slide with anti-fluorescence quenching agent. Fluorescence images were obtained using confocal microscope (FV3000, Olympus, Japan/Stellaris, Leica, Germany).

### RNA Extraction and Quantitative Real-Time PCR

Total RNA was isolated using Trizol Reagent (Vazyme, Nanjing, China) according to the manufacturer's instructions. Collected mRNA was reverse-transcribed to cDNA using HiScript® II Q RT SuperMix kit (Vazyme). Real-time PCR assay was then performed using SYBR green dye (Invitrogen) on StepOne sequence detection system (Applied Biosystems, Waltham, MA, USA). Relative abundance of genes was calculated by using  $2^{-\Delta\Delta CT}$  formula, with  $\beta$ -actin as an internal control. The sequences of the qRT-PCR primers are provided in Supplemental Table S4. PCR Array assay was performed according to the manufacturer's protocol (Wcgene Biotech, Shanghai, China) on StepOne sequence detection system.

### Statistical analysis

All of the values presented on the graphs are given as means  $\pm$  S.E.M. ANOVA and unpaired Student's t-tests were used to analyze the statistical significance. Statistical differences were defined as significant for \* $p < 0.05$  and highly significant for \*\* $p < 0.01$  and \*\*\* $P < 0.001$ . GraphPad Prism5 Demo (GraphPad Software Inc., La Jolla, CA, USA) was used for statistical analysis.

### Results

#### Combination of $\beta$ -glucan and SPIO induces trained immunity to protect mice against sepsis

We determined the therapeutic effect of SPIO and  $\beta$ -glucan to induce trained immunity against sepsis by using the well-established sepsis mouse model. Mice injected with normal saline (group c-E),  $\beta$ -glucan (group b-E), SPIO (group s-E), or  $\beta$ -glucan combined with SPIO (group bs-E) twice a week were then administered with a non-lethal dose of clinical *Escherichia coli* (*E. coli*<sup>a</sup>) (Figure 1A); mice injected intraperitoneally with normal saline were used as controls. Cloning assay showed that bacterial burden of peripheral blood and peritoneum was slightly decreased in mice treated with SPIO, while significantly decreased in mice treated with  $\beta$ -glucan or with the combination of  $\beta$ -glucan and SPIO (Figure 1B). Moreover, treatment with combined  $\beta$ -glucan and SPIO decreased the inflammatory cell infiltration and hyperemia in the alveolar walls (Figure 1C, D). The treatment also decreased the vacuolization and sinusoidal congestion in the liver (Figure 1E, F). These data revealed that the treatment with combined  $\beta$ -glucan and SPIO was superior to  $\beta$ -glucan or SPIO alone in preventing mice against sepsis.

#### Synthesis and characterization of BSNPs

Next, we synthesized  $\beta$ -glucan coupled with SPIO (BSNPs) to optimize treatment, test application of nanomaterials, and provide a convenient and visual basis for the systemic delivery of  $\beta$ -glucan (Figure 2A). Dynamic Light Scattering showed that the hydration particle size of BSNPs was slightly increased to 30 nm (Figure 2B), and its zeta potential was -34 mV (Figure 2C, Supplemental Table S5). Fourier transform infrared spectroscopy displayed the characteristic peaks of  $\beta$ -glucan and iron oxide core in BSNPs (Figure 2D). TEM images revealed a homogeneous dispersion of spherical BSNPs with an average diameter of 8 nm, approximately the same as SPIO (Figure 2E). These data confirmed the successful synthesis of BSNPs.

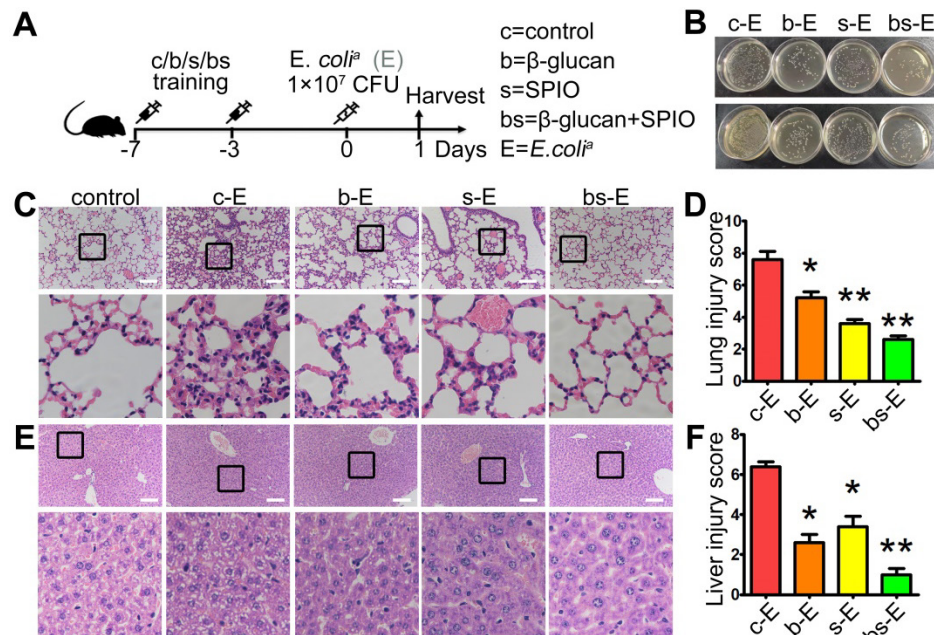


**Figure 1. Trained immunity prevents mice against sepsis in vivo.** (A) Schematic of sepsis after trained immunity experimental setup (n = 5). (B) Blood (upper) and peritoneal lavage fluid (lower) from mice 24 h after infection was plated for 16 h. Representative plate shows bacterial colonies. Representative H&E staining of (C) lung sections or (E) liver sections. Scale bars, 100 μm. Histological injury of (D) lungs and (F) livers in different groups scored as described in Materials and Methods. Data are shown as mean ± SEM (n = 5). \*P < 0.05; \*\*P < 0.01.

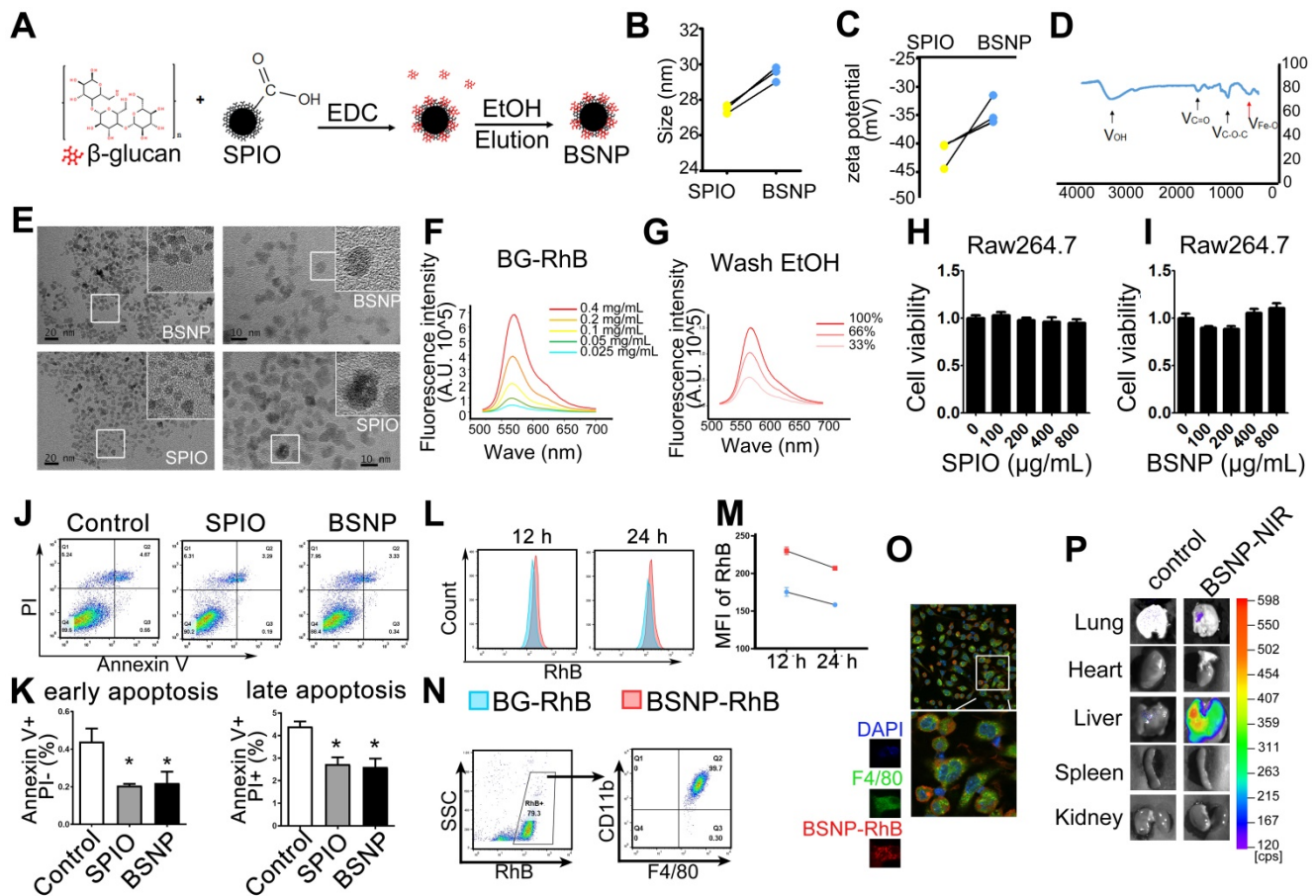


**Figure 2. Characteristic and cytotoxicity of BSNPs.** (A) Schematic of BSNPs synthesis. (B) Hydrate particle size and (C) zeta potential of SPIO and BSNPs. (D) Fourier transform infrared spectroscopy profile of BSNPs. (E) TEM images of SPIO and BSNPs. Scale bar, (left) 20 nm, (right) 10 nm. (F) Spectrum of fluorescence-glugan (BG-RhB) and (G) washing ethanol of fluorescence-BSNPs (BSNP-RhB) with different concentration detected as described in Materials and Methods. (H-I) Raw264.7 cells were treated with different concentration of SPIO or BSNPs for 24 h, cell viability was measured by CCK-8 assay. (J-K) Raw264.7 cells were treated with SPIO at 200 μg/mL for 24 h and cell apoptosis was measured by flow cytometry. (L-N) Mice were injected intraperitoneally with BG-RhB or BSNP-RhB and then sacrificed for peritoneal cells. The fluorescence intensity was measured by flow cytometry at 12 h and 24 h and (O) confocal microscope at 24 h. (P) Mice were injected intraperitoneally with BSNP-NIR for 24 h. The ex vivo imaging of major organs was carried out on the *In vivo* Imaging System. Data are shown as mean ± SEM (n = 3). \*P < 0.05.

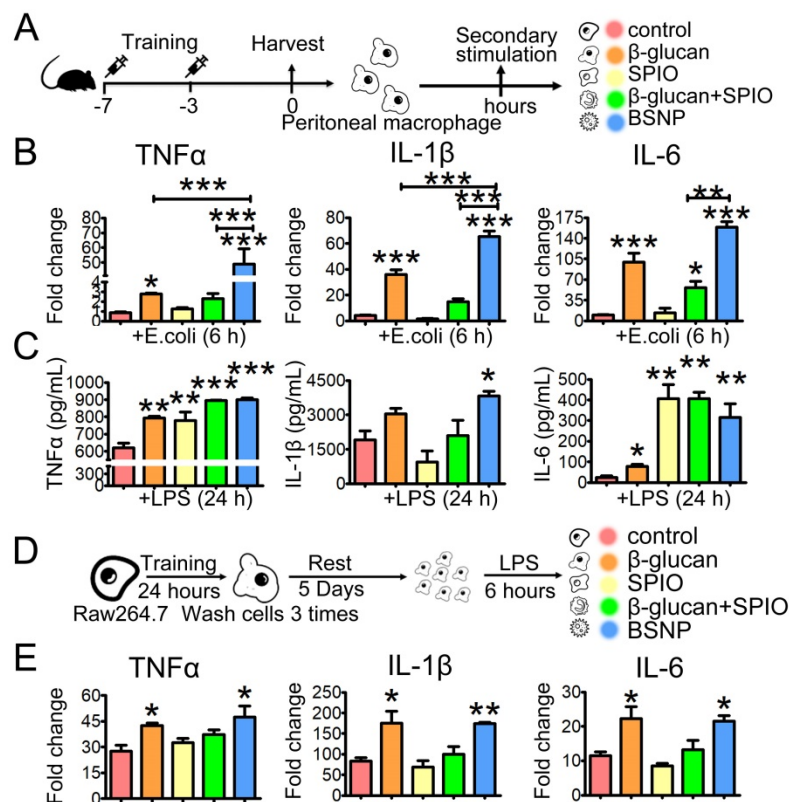


**Figure 3. Trained immunity in macrophages alters the expressions of inflammatory cytokines under secondary stimulation. (A)** Schematic of *ex vivo* trained immunity experimental setup ( $n = 3$ ). After treatment, peritoneal macrophages were obtained and rest overnight before secondary stimulation. **(B)** Fold changes of inflammatory cytokines were determined by quantitative PCR at 6 h after macrophages treated with *E. coli*. **(C)** Cytokines production in cells was determined by ELISA at 24 h after LPS treatment. **(D)** Schematic of *in vitro* trained immunity experimental setup. **(E)** Fold changes of inflammatory cytokines were determined by quantitative PCR at 6 h after LPS stimulation. Data are shown as mean  $\pm$  SEM ( $n = 3$ ). \* $P < 0.05$ ; \*\* $P < 0.01$ ; \*\*\* $P < 0.001$ .

We prepared fluorescence-labeled  $\beta$ -glucan (BG-RhB) to synthesize fluorescence-labeled BSNPs (BSNP-RhB) for the quantitative analysis of  $\beta$ -glucan. The spectrum of different concentrations of BG-RhB (Figure 2F) and the eluted ethanol containing the unbound BG-RhB were determined by Full-function Fluorescence Spectrometry (Figure 2G) (Supplemental Table S2). The mass ratio of  $\beta$ -glucan and SPIO on BSNP was 3:20, as calculated by the standard curve. When Raw264.7 cells were treated with different concentrations of SPIO or BSNPs for 24 h, cell viability was not affected even under the highest concentration at 800  $\mu\text{g}/\text{mL}$  (Figure 2H-I). Flow cytometry showed that apoptosis of Raw264.7 cells was slightly decreased after SPIO and BSNP treatment (Figure 2J-K).

Mice were intraperitoneally injected with BG-RhB or BSNP-RhB to monitor the efficiency of macrophage internalization. The mice were then sacrificed to obtain peritoneal macrophages, and fluorescence intensity was determined by flow cytometry. High fluorescence intensity was detected in the BSNP-RhB group at 12 h and 24 h after BSNPs treatment, slightly declining in both groups at 24 h (Figure 2L-M). Almost all BSNP-RhB positive cells were CD11b $^+$  F4/80 $^+$  macrophages (Figure 2N-O),

indicating that the macrophages could ingest more BSNPs that were degraded slower than  $\beta$ -glucan. Moreover, *ex vivo* imaging of dissected tissues showed localization of BSNPs in the lungs and livers of septic mice (Figure 2P). The images from confocal microscopy revealed colocalization of F4/80 $^+$  macrophages and BSNP-RhB in the liver (Supplementary Figure S1). These data verified that BSNPs could accumulate in the damaged organs and be ingested by macrophages efficiently.

### BSNP-induced trained immunity promotes immune responses of macrophages

Trained immunity results in strong reaction of the innate immune system under sterile triggers of inflammation or secondary infections, enhancing protection against tumors [37-38] and sepsis [39-40]. To evaluate whether BSNPs could induce trained immunity in macrophages, peritoneal macrophages and bone marrow-derived macrophages (BMDM) were obtained from the trained immunity mice and then stimulated with *E. coli* *ex vivo* (Figure 3A, Supplementary Figure S2A). Consistent with the previous study [41-42],  $\beta$ -glucan treatment enhanced TNF $\alpha$ , IL-1 $\beta$ , and IL-6 mRNA expression (Figure 3B). SPIO treatment had little effect on these inflammatory

factors, while BSNP treatment significantly raised their mRNA expression (Figure 3B, Supplementary Figure S2B). Moreover, TNF $\alpha$ , IL-1 $\beta$ , and IL-6 were significantly higher inside BSNP-treated cells than other treatments (Figure 3C, Supplementary Figure S2C), suggesting that BSNP treatment enhanced the production of pro-inflammatory cytokines by macrophages. Similar results were obtained using the macrophage cell line Raw264.7 (Figure 3D-E). Collectively, these data indicated that BSNP-induced trained immunity could induce the expression of inflammatory cytokines by macrophages, which could be a powerful defense strategy against bacterial infection.

### BSNP-induced trained immunity enhances phagocytosis by macrophages

Besides inflammatory cytokines, phagocytosis by macrophages is another defense strategy against bacterial infection, while impaired macrophage phagocytosis is often related to poor prognosis of sepsis [43,44]. Therefore, we tested phagocytosis by peritoneal macrophage from each group to further explore the superiority of BSNPs. *E. coli*<sup>Δ</sup> were stained with pHrodo, and co-cultured with macrophages for 1 h. Fluorescence green appeared only when bacteria were phagocytosed by macrophages. Mice and Raw264.7 cells were treated the same as described before (Figure 3A, 3D). Results showed that BSNP treatment promoted macrophages to phagocytose *E. coli*<sup>Δ</sup>. The mean fluorescence intensity of BSNP and the combined treatment groups was much stronger than the  $\beta$ -glucan or SPIO group (Figure 4A). Similar

results were also obtained from the trained immunity model *in vitro* (Figure 4B). Moreover, immunofluorescence images showed more *E. coli*<sup>Δ</sup> in BSNP-treated macrophages (Figure 4C).

These data indicated that BSNP treatment could induce macrophages to engulf more pathogens. Therefore, we co-cultured BMDMs from mice with *E. coli*-pHrodo for 1 h to test primary phagocytosis. Subsequently, the cells were washed 3 times and cultured with fresh medium for another 2 h to monitor the digestion of bacteria. Fluorescence intensity was higher in the BSNP group than the control group at 1 h, indicating that BSNP promoted macrophages to phagocytose bacteria. Fluorescence intensity in the BSNP group was lower after another 2 h because BSNPs enhanced the digestion of macrophages (Supplementary Figure S2). Collectively, our results indicated that BSNPs could train macrophages into a more active state.

### BSNP-induced trained immunity prevents mice against sepsis

Next, we aimed to investigate the preventive effect of BSNPs. Mice were treated with BSNPs (group n-E) or  $\beta$ -glucan combined with SPIO (group bs-E), followed by the intraperitoneal injection with *E. coli*<sup>Δ</sup>. We used a higher dose of *E. coli*<sup>Δ</sup> to better judge the therapeutic difference between BSNP treatment and combined treatment (Figure 5A). The BSNP-treated mice had a less bacterial burden in the blood and peritoneum than any other group (Figure 5B). BSNP treatment decreased incrustation and hyperemia in the alveolar walls (Figure 5E-F) and decreased

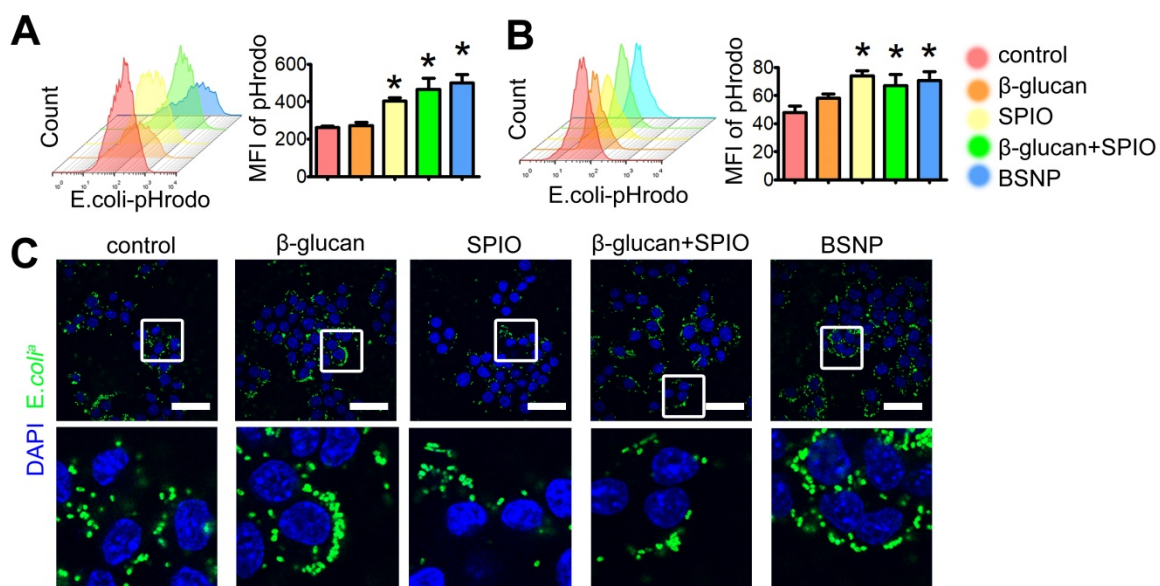


**Figure 4.** Trained immunity promotes macrophages to phagocytose bacteria. Mice and Raw264.7 cells were treated as described in Materials and methods section. After treatment, macrophages were obtained and rest overnight before co-cultured with pHrodo labeled *E. coli*<sup>Δ</sup> for 1 h. Phagocytosis of (A) peritoneal macrophages from each group was determined by flow cytometry. Phagocytosis of Raw264.7 cells from each group was determined by (B) flow cytometry and (C) confocal microscope. Scale bars, 30  $\mu$ m. Data are shown as mean  $\pm$  SEM (n = 3). \*P < 0.05.

sinusoidal congestion in the liver (Figure 5G-H). Importantly, when injected with a lethal dose of *E. coli*<sup>a</sup>, BSNPs treatment improved the survival rate to 100% (Figure 5C-D). These data indicated that BSNPs were superior to  $\beta$ -glucan and SPIO in preventing mice against *E. coli*-induced sepsis.

To further confirm the superior effect of BSNPs, we used the well-established cecal ligation and puncture (CLP) sepsis model. Mice treated with BSNPs (N-CLP) or  $\beta$ -glucan combined with SPIO (BS-CLP) were sacrificed at 24 h after CLP operation. Mice maintained a stable body weight during modeling while losing weight after CLP (Supplementary Figure S3). Also, mice treated with BSNPs had a less bacterial burden in blood and peritoneum than the CLP and BS-CLP groups (Figure 5I), and the TNF $\alpha$ , IL-1 $\beta$ , and IL-6 levels were elevated in the sera of CLP mice. While IL-1 $\beta$  and IL-6 were slightly decreased in the BS-CLP group, there was a remarkable decrease in the BSNP group (Figure 5J-K), and the TNF $\alpha$  level also showed the same tendency (Figure 5L). BSNP treatment decreased incrustation, hyperemia, and exudates in the alveolar walls (Figure 5O-P) and decreased sinusoidal congestion, vacuolization, and infiltration of

neutrophils in the liver (Figure 5Q-R). The biochemical analysis also showed that liver damage markers, such as aspartate aminotransferase (AST) and alanine aminotransferase (ALT), were significantly decreased in the BSNP group (Figure 5M-N). These data confirmed that BSNP-induced trained immunity could better prevent mice from sepsis.

### BSNP-induced trained immunity protects mice against secondary infection

Inflammation in sepsis results in ablation of resident macrophages such as peritoneal macrophages [45-46], and depletion of macrophages is associated with poor prognosis [47-48]. Also, patients with sepsis are more sensitive to secondary infections, resulting in high mortality and recurrence rate [49-50]. To explore the therapeutic potential of BSNP on secondary infections, we established a sepsis model before treatment (Figure 6A). Peritoneal macrophages in mice were reduced at day 7 after primary infection. Macrophages were increased when mice were treated with BSNPs compared with those treated with combined  $\beta$ -glucan and SPIO (Figure 6B-C). Large peritoneal macrophages (LPMs) and

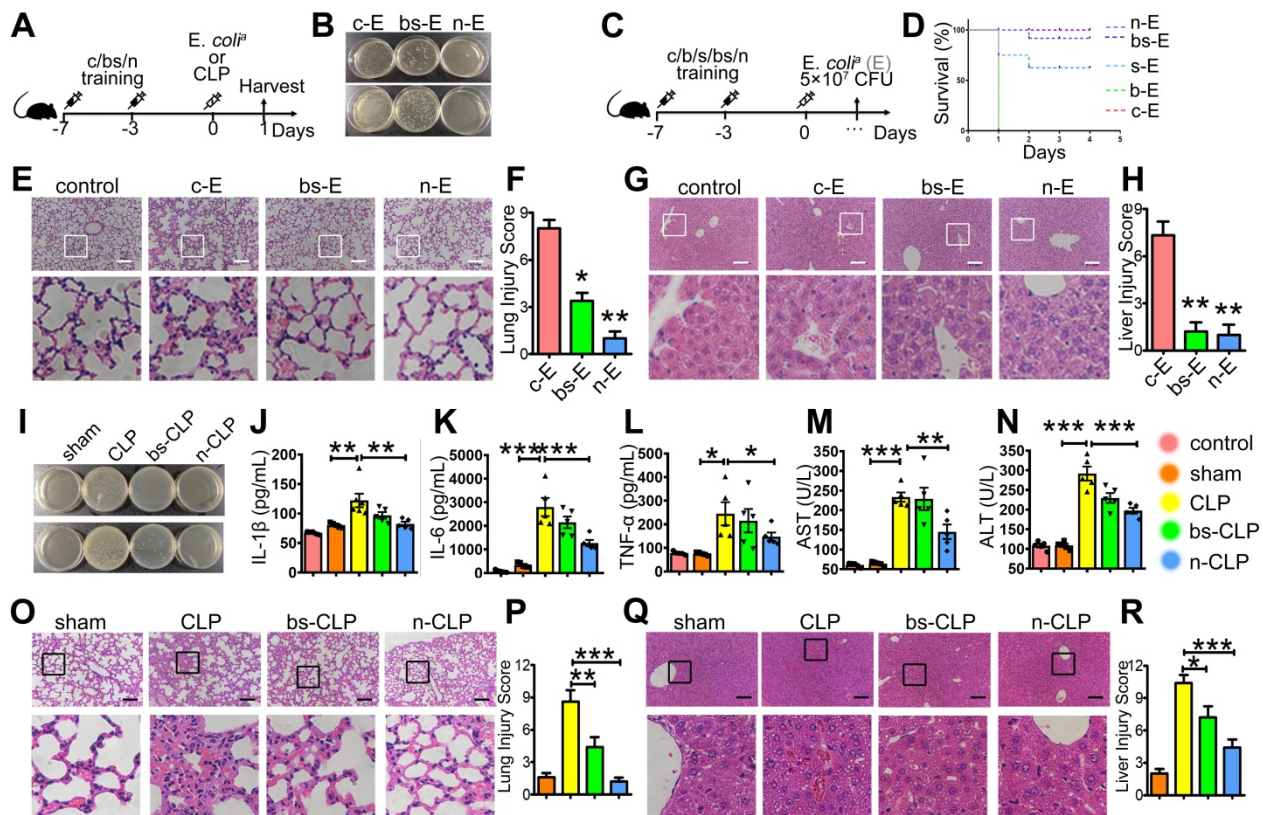


**Figure 5. BSNP-induced trained immunity prevents mice against sepsis.** (A) Schematic of *in vivo* trained immunity experimental setup (n = 5). (B, I) Blood (upper) and peritoneal lavage fluid (lower) from mice 24 h after infection was plated for 16 h. Representative plate shows bacterial colonies. (C) Schematic for survival curve experimental setup (n = 9). (D) Survival curve of mice from each group after injected with lethal dose of *E. coli*<sup>a</sup>. Representative H&E staining of (E, O) lung sections or (G, Q) liver sections. Scale bars, 100  $\mu$ m. Histological injury of (F, P) lungs and (H, R) livers in different groups scored as described in Materials and Methods. (J-L) Cytokines levels in serum was determined by ELISA. (M, N) Biochemical analysis of serum concentrations of ALT and AST. Data are shown as mean  $\pm$  SEM (n = 5) \*P < 0.05; \*\*P < 0.01; \*\*\*P < 0.001.

small peritoneal macrophages (SPMs) are two main subsets of peritoneal macrophages. LPMs, originating from embryogenic precursors stay in enterocoelia under steady conditions. Conversely, SPMs, originating from peripheral monocytes, only increase under inflammatory conditions. When mice were injected with *E. coli*, LPMs vanished within 2 days following which SPMs infiltrated in enterocoelia as replenishment. BSNPs promoted the transformation of SPMs to LPMs, accelerating the homeostasis of peritoneal macrophages (Supplementary Figure S4).

We established a double-infection model to better explore the BSNP effect under a clinical scenario (Figure 6D). Compared with the single-infection septic model, lung injury in the double-infection model was much more severe with thicker alveolar walls, more pulmonary hemorrhage, and added pulmonary debris. BSNP treatment remarkably promoted the clearance of bacteria (Figure 6E). The lung injury score of BSNP-treated mice was less than the double-infected mice, combined treatment mice, and single-infected mice (Figure 6F, H). Liver injury in the double-infection model was also much severe when compared with the single-infection model in terms of aggravated sinusoidal congestion and vacuolization. While the liver injury score was unchanged by the combined

treatment of  $\beta$ -glucan and SPIO, it was remarkably reduced by BSNP treatment (Figure 6G, I). Thus, BSNPs were better able to promote macrophage recovery after primary bacterial infection and protect mice against secondary infection. Our data indicated that BSNPs were beneficial for the clearance of bacteria and reversion of immune paralysis.

### BSNP-induced trained immunity occurs in an mTOR-dependent manner

Previous studies have shown that the mTOR signaling pathway is central to the development of trained immunity [18]. To investigate the mechanism underlying the superior therapeutic efficacy of BSNPs, we examined the phosphorylation of upstream and downstream proteins S6 and 4EBP in the mTOR pathway using the *in vitro* trained immunity model with macrophage cell line Raw264.7 (Figure 7A). Akt, S6, and 4EBP phosphorylation levels increased after BSNP treatment than after  $\beta$ -glucan treatment, but there was no significant difference in S6 and 4EBP phosphorylation levels between the two groups. While SPIO treatment and combined treatment with  $\beta$ -glucan and SPIO did not affect the phosphorylation of Akt, the phosphorylation of S6 and 4EBP was up-regulated (Figure 7B-C).

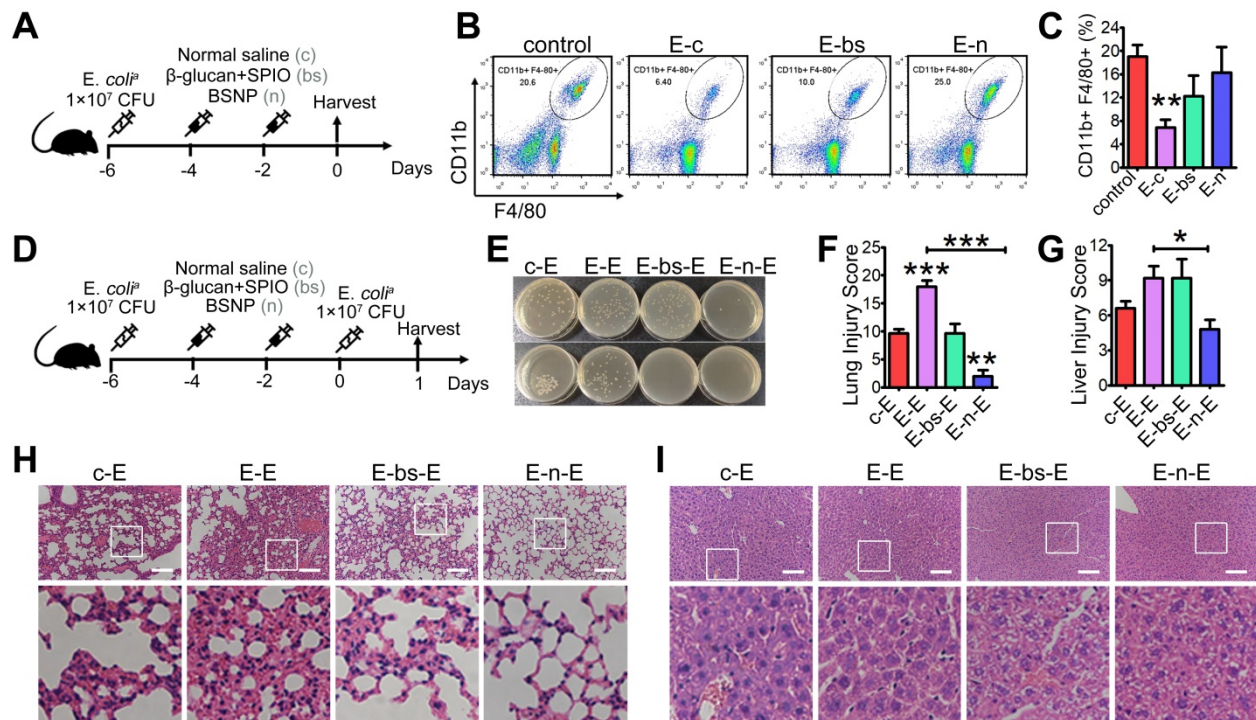


**Figure 6. BSNP-induced trained immunity protects mice against secondary infection.** (A) Schematic of *in vivo* phagocytic test experimental setup (n = 3). (B-C) Macrophages (CD11b+, F4/80+ subset) in peritoneal cells from each group were determined by flow cytometry. (D) Schematic of double-infection experimental setup (n = 5). (E) Blood (upper) and peritoneal lavage fluid (below) from mice 24 h after secondary infection was plated for 16 h. Representative plate shows bacterial colonies. Representative H&E staining of (H) lung sections and (I) liver sections. Scale bars, 100  $\mu$ m. Histological injury of (F) lungs and (G) livers in different groups scored as described in Materials and Methods. Data are shown as mean  $\pm$  SEM (n = 5). \*P < 0.05; \*\*P < 0.01; \*\*\*P < 0.001.

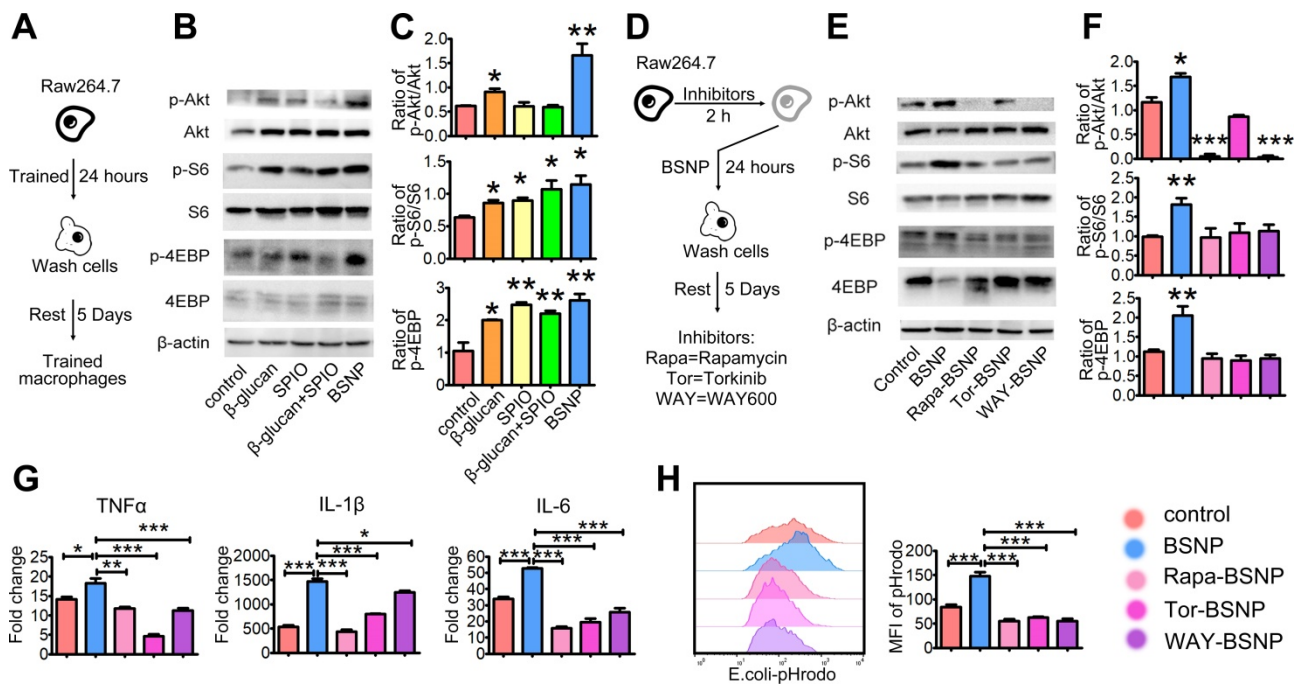


**Figure 7. BSNP-induced trained immunity is in an mTOR dependent manner.** (A) Schematic of *in vitro* trained immunity experimental setup. Cells were lysed after 5 days of rest. (B-C, E-F) Expression of proteins downstream mTOR pathway were determined by western blot. (D) Schematic of *in vitro* BSNP-induced trained immunity experimental setup. Raw264.7 cells were treated with mTOR inhibitor Rapamycin (10 μmol/L), Torkinib (200 nmol/L), or WAY600 (200 nmol/L) 2 h previous to BSNPs treatment. (G) Fold changes of inflammatory cytokines were determined by quantitative PCR at 6 h after LPS stimulation. (H) Phagocytosis of Raw264.7 cells from each group was determined by flow cytometry. Data are shown as mean ± SEM (n = 3). \*P < 0.05; \*\*P < 0.01; \*\*\*P < 0.001.

Next, we treated Raw264.7 cells with mTOR inhibitors 2 h before BSNP treatment. Rapamycin, Torkinib, and WAY600 were used to inhibit the activity of mTOR complex1, complex 1 and 2, and the assembly of mTOR complex 1/2, respectively (Figure 7D). BSNP-induced phosphorylation of Akt, S6, and 4EBP was inhibited by Rapamycin, Torkinib, and WAY600 (Figure 7E-F). Subsequently, Raw264.7 cells treated with mTOR inhibitors followed by BSNPs were stimulated by LPS for 6 h. The upregulation of TNFα, IL-1β, and IL-6 was significantly decreased by these inhibitors (Figure 7G). Furthermore, macrophages from each group were co-cultured with *E. coli*<sup>Δ</sup>-pHrodo for 1 h. Flow cytometry showed that BSNP-induced phagocytosis was also significantly decreased by these inhibitors (Figure 7H). These data suggested that BSNP-induced trained immunity was mTOR dependent.

Finally, we performed a PCR array on peritoneal macrophages from control mice or BSNP-treated mice to analyze the gene expression pattern in the mTOR signaling pathway (Figure 8A-B). More genes were up-regulated than down-regulated after BSNP treatment (Figure 8C). Among genes with significant fold-change (Figure 8D, Supplementary Figure S5), *Igf1* and *Sesn1* were the most up-regulated and *Vegfa* and *Rps6ka5* were the most down-regulated genes. After BSNPs treatment, active signaling pathways were analyzed using the KEGG pathway database (Figure 8E), and biological process and molecular

functions were analyzed by Gene Ontology enrichment analysis (Figure 8F-G, Supplementary Figure S6).

Our data revealed a different gene expression profile in macrophages after BSNP treatment. When genes participating in mTOR signaling were investigated, *Igf1* and *Eif4ebp1* were identified as master regulators. Besides the mTOR signaling pathway, BSNP treatment also activated AMPK, PI3K/Akt, and proteoglycan signaling pathways. Thus, BSNP treatment mainly regulated cellular signal transduction, protein modification, and cell cycle progression via regulating ATP binding and the kinase activity.

## Discussion

As an emerging drug delivery system, nanoparticles have unlimited potential. It has been shown that SPIO engineered to escape the immune recognition could be less taken up by macrophages, thereby lengthening the retention time of SPIO [51] and reducing the inflammation induced by SPIO [52]. Combining small molecule drugs or antibodies with SPIO could reduce their toxicity and increase their efficacy [53]. In the present study, we successfully synthesized novel BSNPs by coupling β-glucan and SPIO, significantly reducing the dose of β-glucan from 500 μg per mouse to 22.5 μg on BSNPs per mouse for inducing trained immunity and lowering the possible toxicity.

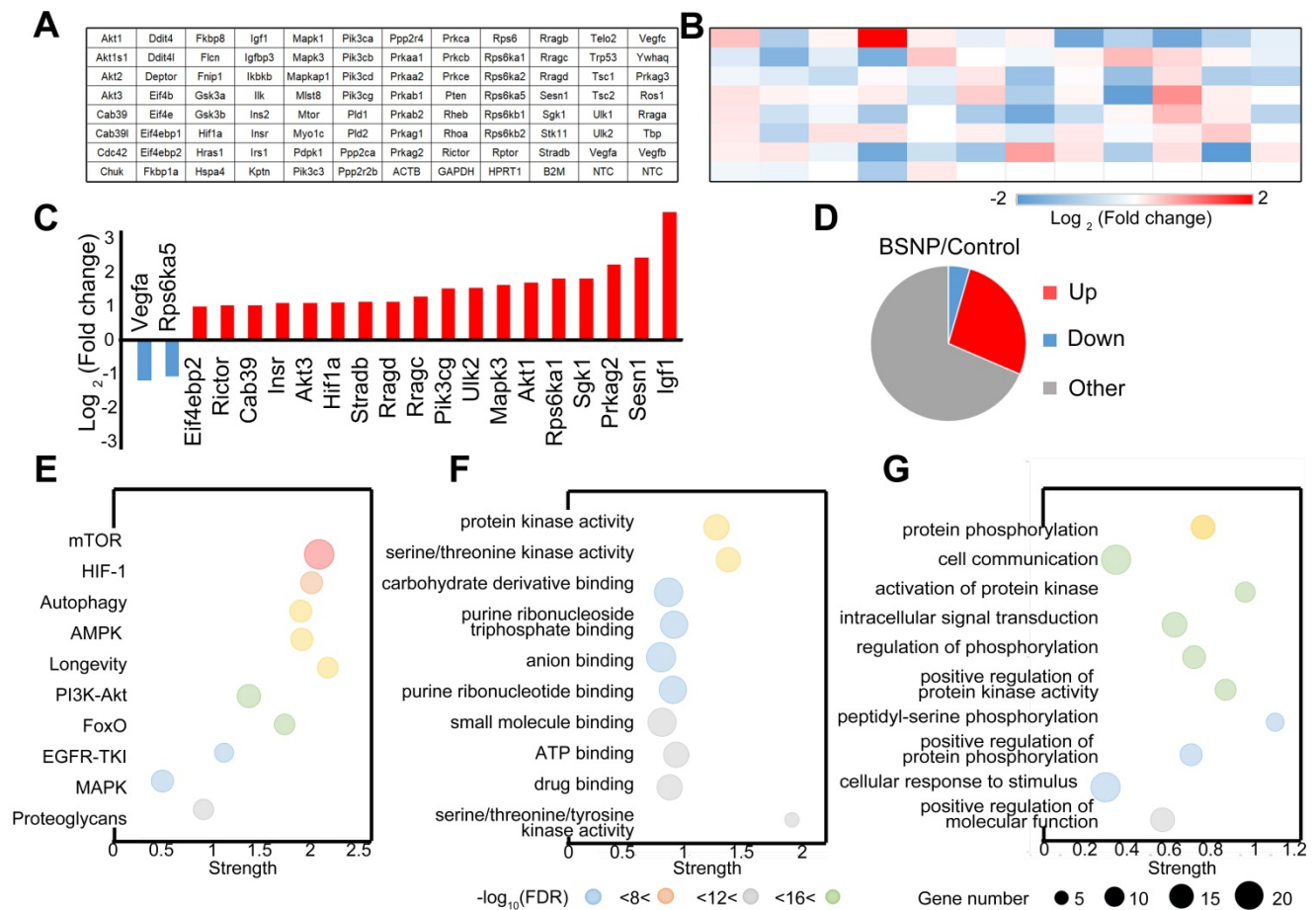


**Figure 8. Expression pattern of mTOR pathway related genes in trained immunity macrophages from BSNP-treated mice. (A)** Plate layout of PCR array. **(B)** Heat map showed fold changes of genes in macrophages from BSNPs treated mice versus control mice. **(C)** Major differentially regulated mTOR pathway genes. **(D)** Pie chart displayed number of differentially regulated genes. **(E-G)** Enriched GO categories of major differentially regulated genes in (E) neighborhood signaling pathway, (F) biological process and (G) functions.

We performed *in vitro* and *in vivo* experiments and found that BSNP treatment was superior to  $\beta$ -glucan in promoting macrophages to produce cytokines *in vivo* but not *in vitro*. Macrophages from BSNP-treated mice produced more inflammatory cytokines than  $\beta$ -glucan-treated mice, but there was no significant difference in Raw264.7 cells between BSNP and  $\beta$ -glucan. These observations indicated that BSNP uptake by peritoneal macrophages in mice was improved compared to cultured macrophages due to the coupling of  $\beta$ -glucan with SPIO and also because the characteristics of peritoneal macrophages were different from Raw264.7 cells. Thus, our study showed that nanoparticles were easier for uptake by macrophages *in vivo* than *in vitro*.

While exploring the mechanism of BSNP-induced trained immunity, we examined the hepcidin-ferroportin iron metabolism pathway closely associated with inflammation, infection [54-55] and sepsis [56-57]. Although the  $\beta$ -glucan treatment had little effect on ferroportin1, SPIO could significantly raise ferroportin1 (FPN1) expression (Supplementary Figure S7A). However, in our study,

treatment with  $\beta$ -glucan, SPIO, or combined  $\beta$ -glucan and SPIO protected FPN1-deficient mice against sepsis, manifested by reduced blood bacterial burden and lung damage (Supplementary Figure S7B-E). These results suggested that  $\beta$ -glucan and SPIO treatment effects were independent of the classical iron metabolism pathway. Also, lipocalin-2 is considered as a standby iron transporter under FPN1 deficiency [58]. In lipocalin-2-deficient mice, brain injury caused by LPS was severer than normal mice [59]. However, lipocalin-2 protein expression and secretion were not different among  $\beta$ -glucan-, SPIO-, combined  $\beta$ -glucan-SPIO-, or BSNP-treated macrophages (Supplementary Figure S8). These data suggested that BSNP-induced trained immunity was likely independent of lipocalin-2. Thus, the link between iron metabolism and trained immunity remains unclear.

Previous studies reported that  $\beta$ -glucan-induced trained immunity induced macrophages to produce more inflammatory cytokines under secondary stimulation [60-61]. Inflammation is a double-edged sword, as it results in tissue injury but is also

necessary for host defense. We speculated that BSNPs could serve as an immunostimulatory agent, protecting the host against primary and secondary infections [62-63]. Activation and M1 polarization of macrophages are beneficial for bacterial clearance and survival rate of infected mice [64-65]. The way to balance inflammation and antibacterial activity of macrophages needs to be further studied.

In the present study, we found that inflammatory cytokine levels inside and outside the macrophages were different. After LPS stimulation for 24 h, inflammatory cytokine levels in the supernatant of macrophages obtained from BSNP-treated mice were similar to non-treated mice (Supplementary Figure S9). The data (Figure 3) suggested that BSNP-induced trained immunity could induce macrophages to produce but not secrete inflammatory cytokines. Furthermore, after treatment for 6 days,  $\beta$ -glucan induced M1 polarization, while combined  $\beta$ -glucan and SPIO and BSNPs reduced M1 polarization. On the contrary,  $\beta$ -glucan, SPIO, combined  $\beta$ -glucan and SPIO, or BSNPs had little effect on M2 polarization (Supplementary Figure S10). It is conceivable that the BSNP effect on macrophage polarization is conducive to killing bacteria inside macrophages while reducing the damage to adjacent cells. In summary, our study provided strong evidence for increased macrophage phagocytosis of bacteria via BSNP-induced trained immunity.

## Conclusions

We successfully synthesized novel nanoparticles, BSNPs, by coupling  $\beta$ -glucan and SPIO and found that BSNPs could be taken up by macrophages and induced trained immunity efficiently. BSNPs induced macrophages to produce inflammatory cytokines and accelerated the clearance of bacteria by phagocytosis. BSNP-induced trained immunity could guard against sepsis and also protect against re-infection in the short term. The BSNP-induced trained immunity functioned in an mTOR-dependent manner. Our study provided a new prevention and treatment strategy for sepsis. Furthermore, it offered a theoretical basis for the application of nanomaterials in trained immunity that could be extended to other situations such as severe trauma, pneumonia, and systemic lupus erythematosus.

## Abbreviations

SPIO: superparamagnetic iron oxide; BSNPs:  $\beta$ -glucan coupling SPIO nanoparticles; mTOR: mammalian target of rapamycin; qRT-PCR: quantitative real-time polymerase chain reaction; COVID-19: coronavirus disease 2019; FDA: Food and Drug Administration; IL: interleukin; TNF: tumour

necrosis factor; LPS: lipopolysaccharide; RhB: Rhodamine B isothiocyanate; EDC: 1-ethyl-3-(3-dimethylaminopropyl) carbodiimide hydrochloride; DMEM: Dulbecco's modified Eagle's medium; ELISA: Enzyme Linked Immunosorbent Assay; SDS-PAGE: sodium dodecyl sulfate polyacrylamide gel electrophoresis; PVDF: poly(1,1-difluoroethylene); PFA: paraformaldehyde; H&E: hematoxylin-eosin; EtOH: ethyl alcohol; MFI: mean fluorescence intensity; DAPI: 4,6-diamino-2-phenyl indole; CD11b: integrin Alpha M; F4/80: mouse EGF-like module-containing mucin-like hormone receptor-like 1; BMDM: bone marrow derived macrophages; LPM: Large peritoneal macrophages; SPM: small peritoneal macrophages.

## Supplementary Material

Supplementary figures and tables.

<https://www.thno.org/v12p0675s1.pdf>

## Acknowledgements

This work was supported by National Key Research and Development Program of China (2017YFA0104303), the Key Research and Development Program of Jiangsu Province (BE2019706), Fund of Biosecurity Specialized Project of PLA (NO. 19SWAQ18), and innovative research project for doctoral students of Nanjing University (CXC19-45).

## Author Contributions

All authors were involved in drafting the article or revising it critically for important intellectual content, and all authors approved the final version to be published. Y. Hou, H. Dou, K. Li, H. Liang and Y. Pan conceived and designed the study. Y. Pan performed all major experiments with help from J. Li, X. Xia, J. Wang in experiments on mice, and help from Q. Jiang, J. Yang in experiments on cells. We thank Prof. Ning Gu from Southeast University for providing us SPIO; A/Prof. Hongye Fan from China Pharmaceutical University for advice in establishing mice models; Dr. Yuan Cheng from Nanjing University for advice in synthesis and tracing of nanoparticles.

## Competing Interests

The authors have declared that no competing interest exists.

## References

- [1] Fleischmann-Struzek C, Mellhammar L, Rose N, Cassini A, Rudd KE, Schlattmann P, et al. Incidence and mortality of hospital- and ICU-treated sepsis: results from an updated and expanded systematic review and meta-analysis. *Intensive Care Med.* 2020; 46(8): 1552-1562.
- [2] Markwart R, Saito H, Harder T, Tomczyk S, Cassini A, Fleischmann-Struzek C, et al. Epidemiology and burden of sepsis acquired in hospitals and

- intensive care units: a systematic review and meta-analysis. *Intensive Care Med.* 2020; 46(8): 1536-1551.
- [3] Baghdadi JD, Brook RH, Uslan DZ, Needleman J, Bell DS, Cunningham WE, et al. Association of a care bundle for early sepsis management with mortality among patients with hospital-onset or community-onset sepsis. *JAMA Intern Med.* 2020; 180(5): 707-716.
- [4] Cecconi M, Evans L, Levy M, Rhodes A. Sepsis and septic shock. *Lancet.* 2018; 392(10141): 75-87.
- [5] Reinhart K, Daniels R, Kissoon N, Machado FR, Schachter RD, Finfer S. Recognizing sepsis as a global health priority - a WHO resolution. *N Engl J Med.* 2017; 377(5): 414-417.
- [6] Fernando SM, Rochweg B, Seely AJE. Clinical implications of the third international consensus definitions for sepsis and septic shock (Sepsis-3). *CMAJ.* 2018; 190(36): E1058-E1059.
- [7] Almansa R, Ortega A, Ávila-Alonso A, Heredia-Rodríguez M, Martín S, Benavides D, et al. Quantification of immune dysregulation by next-generation polymerase chain reaction to improve sepsis diagnosis in surgical patients. *Ann Surg.* 2019; 269(3): 545-553.
- [8] Fleischmann C, Scherag A, Adhikari NK, Hartog CS, Tsaganos T, Schlattmann P, et al. Assessment of global incidence and mortality of hospital-treated sepsis. Current Estimates and Limitations. *Am J Respir Crit Care Med.* 2016; 193(3): 259-272.
- [9] Lin GL, McGinley JP, Drysdale SB, Pollard AJ. Epidemiology and immune pathogenesis of viral sepsis. *Front Immunol.* 2018; 9: 2147.
- [10] Li H, Liu L, Zhang D, Xu J, Dai H, Tang N, et al. SARS-CoV-2 and viral sepsis: observations and hypotheses. *Lancet.* 2020; 395(10235): 1517-1520.
- [11] Zhang C, Shi L, Wang FS. Liver injury in COVID-19: management and challenges. *Lancet Gastroenterol Hepatol.* 2020; 5(5): 428-430.
- [12] Alhazzani W, Møller MH, Arabi YM, Loeb M, Gong MN, Fan E, et al. Surviving sepsis campaign: guidelines on the management of critically ill adults with Coronavirus Disease 2019 (COVID-19). *Intensive Care Med.* 2020; 46(5): 854-887.
- [13] Netea MG, Joosten LA, Latz E, Mills KH, Natoli G, Stunnenberg HG, et al. Trained immunity: a program of innate immune memory in health and disease. *Science.* 2016; 352(6284): aaf1098.
- [14] Mantovani A, Netea MG. Trained innate immunity, epigenetics, and Covid-19. *N Engl J Med.* 2020; 383(11): 1078-1080.
- [15] Saeed S, Quintin J, Kerstens HH, Rao NA, Aghajani-farah A, Matarese F, et al. Epigenetic programming of monocyte-to-macrophage differentiation and trained innate immunity. *Science.* 2014; 345(6204): 1251086.
- [16] Ciarlo E, Heinonen T, Théroutte C, Asgari F, Le Roy D, Netea MG, et al. Trained immunity confers broad-spectrum protection against bacterial infections. *J Infect Dis.* 2020; 222(11): 1869-1881.
- [17] Paris S, Chapat L, Martin-Cagnon N, Durand PY, Piney L, Cariou C, et al.  $\beta$ -glucan as trained immunity-based adjuvants for rabies vaccines in dogs. *Front Immunol.* 2020; 11: 564497.
- [18] Cheng SC, Quintin J, Cramer RA, Shephardson KM, Saeed S, Kumar V, et al. mTOR- and HIF-1 $\alpha$ -mediated aerobic glycolysis as metabolic basis for trained immunity. *Science.* 2014; 345(6204): 1250684.
- [19] Moorlag SJCFM, Khan N, Novakovic B, Kaufmann E, Jansen T, van Crevel R, et al.  $\beta$ -glucan induces protective trained immunity against *Mycobacterium tuberculosis* infection: a key role for IL-1. *Cell Rep.* 2020; 31(7): 107634.
- [20] Geller A, Yan J. Could the induction of trained immunity by  $\beta$ -glucan serve as a defense against COVID-19? *Front Immunol.* 2020; 11: 1782.
- [21] Wang XS, Zeng JY, Li MJ, Li QR, Gao F, Zhang XZ. Highly stable iron carbonyl complex delivery nanosystem for improving cancer therapy. *ACS Nano.* 2020; 14(8): 9848-9860.
- [22] Liu Z, Simchick GA, Qiao J, Ashcraft MM, Cui S, Nagy T, et al. Reactive oxygen species-triggered dissociation of a polyrotaxane-based nanochelator for enhanced clearance of systemic and hepatic iron. *ACS Nano.* 2021; 15(1): 419-433.
- [23] Ying W, Zhang Y, Gao W, Cai X, Wang G, Wu X, et al. Hollow magnetic nanocatalysts drive starvation-chemodynamic-hyperthermia synergistic therapy for tumor. *ACS Nano.* 2020; 14(8): 9662-9674.
- [24] Reichel D, Sagong B, Teh J, Zhang Y, Wagner S, Wang H, et al. Near infrared fluorescent nanopatform for targeted intraoperative resection and chemotherapeutic treatment of glioblastoma. *ACS Nano.* 2020; 14(7): 8392-8408.
- [25] Stoumpos S, Tan A, Hall Barrientos P, Stevenson K, Thomson PC, Kasthuri R, et al. Ferumoxytol MR angiography versus duplex US for vascular mapping before arteriovenous fistula surgery for hemodialysis. *Radiology.* 2020; 297(1): 214-222.
- [26] Yang SJ, Huang CH, Wang CH, Shieh MJ, Chen KC. The synergistic effect of hyperthermia and chemotherapy in magnetite nanomedicine-based lung cancer treatment. *Int J Nanomedicine.* 2020; 15: 10331-10347.
- [27] Shu G, Chen M, Song J, Xu X, Lu C, Du Y, et al. Sialic acid-engineered mesoporous polydopamine nanoparticles loaded with SPIO and Fe<sup>3+</sup> as a novel theranostic agent for T1/T2 dual-mode MRI-guided combined chemo-photothermal treatment of hepatic cancer. *Bioact Mater.* 2020; 6(5): 1423-1435.
- [28] Dong W, Huang A, Huang J, Wu P, Guo S, Liu H, et al. Plasmid-loadable magnetic/ultrasound-responsive nanodroplets with a SPIO-NP dispersed perfluoropentane core and lipid shell for tumor-targeted intracellular plasmid delivery. *Biomater Sci.* 2020; 8(19): 5329-5345.
- [29] Liu Y, Zhao J, Jiang J, Chen F, Fang X. Doxorubicin delivered using nanoparticles camouflaged with mesenchymal stem cell membranes to treat colon cancer. *Int J Nanomedicine.* 2020; 15: 2873-2884.
- [30] Tacke F, Nuraldeen R, Koch A, Strathmann K, Hutschenreuter G, Trautwein C, et al. Iron parameters determine the prognosis of critically ill patients. *Crit Care Med.* 2016; 44(6): 1049-58.
- [31] Shah A, Frost JN, Aaron L, Donovan K, Drakesmith H, Collaborators. Systemic hypoferrinemia and severity of hypoxemic respiratory failure in COVID-19. *Crit Care.* 2020; 24(1): 320.
- [32] Pammi M, Suresh G. Enteral lactoferrin supplementation for prevention of sepsis and necrotizing enterocolitis in preterm infants. *Cochrane Database Syst Rev.* 2020; 3(3): CD007137.
- [33] Xu Y, Li Y, Liu X, Pan Y, Sun Z, Xue Y, et al. SPIONs enhances IL-10-producing macrophages to relieve sepsis via Cav1-Notch1/HES1-mediated autophagy. *Int J Nanomedicine.* 2019; 14: 6779-6797.
- [34] Aziz M, Ode Y, Zhou M, Ochani M, Holodick NE, Rothstein TL, et al. B-1a cells protect mice from sepsis-induced acute lung injury. *Mol Med.* 2018; 24(1): 26.
- [35] Aziz M, Matsuda A, Yang WL, Jacob A, Wang P. Milk fat globule-epidermal growth factor-factor 8 attenuates neutrophil infiltration in acute lung injury via modulation of CXCR2. *J Immunol.* 2012; 189(1): 393-402.
- [36] Hayase N, Doi K, Hiruma T, Matsuura R, Hamasaki Y, Noiri E, et al. Recombinant thrombomodulin on neutrophil extracellular traps in murine intestinal ischemia-reperfusion. *Anesthesiology.* 2019; 131(4): 866-882.
- [37] Kalafati L, Kourtzelis I, Schulte-Schrepping J, Li X, Hatzioannou A, Grinenko T, et al. Innate immune training of granulopoiesis promotes anti-tumor activity. *Cell.* 2020; 183(3): 771-785.e12.
- [38] Priem B, van Leent MMT, Teunissen AJP, Sofias AM, Mourits VP, Willemsen L, et al. Trained immunity-promoting nanobiologic therapy suppresses tumor growth and potentiates checkpoint inhibition. *Cell.* 2020; 183(3): 786-801.e19.
- [39] Dos Santos JC, Barroso de Figueiredo AM, Teodoro Silva MV, Cirovic B, de Bree LCJ, Damen MSMA, et al.  $\beta$ -glucan-induced trained immunity protects against leishmania braziliensis infection: a crucial role for IL-32. *Cell Rep.* 2019; 28(10): 2659-2672.e6.
- [40] Domínguez-Andrés J, Novakovic B, Li Y, Scicluna BP, Gresnigt MS, Arts RJW, et al. The itaconate pathway is a central regulatory node linking innate immune tolerance and trained immunity. *Cell Metab.* 2019; 29(1): 211-220.e5.
- [41] Keating ST, Groh L, van der Heijden CDCC, Rodriguez H, Dos Santos JC, Fanucchi S, et al. The Set7 lysine methyltransferase regulates plasticity in oxidative phosphorylation necessary for trained immunity induced by  $\beta$ -glucan. *Cell Rep.* 2020; 31(3): 107548.
- [42] Arts RJ, Novakovic B, Ter Horst R, Carvalho A, Bekkering S, Lachmandas E, et al. Glutaminolysis and fumarate accumulation integrate immunometabolic and epigenetic programs in trained immunity. *Cell Metab.* 2016; 24(6): 807-819.
- [43] Rabani R, Volchuk A, Jerkic M, Ormesher L, Garces-Ramirez L, Canton J, et al. Mesenchymal stem cells enhance NOX2-dependent reactive oxygen species production and bacterial killing in macrophages during sepsis. *Eur Respir J.* 2018; 51(4): 1702021.
- [44] Roewe J, Stavrides G, Struete M, Sharma A, Marini F, Mann A, et al. Bacterial polyphosphates interfere with the innate host defense to infection. *Nat Commun.* 2020; 11(1): 4035.
- [45] Nelson DS. Reaction to antigens *in vivo* of the peritoneal macrophages of guinea-pigs with delayed type hypersensitivity. Effects of anticoagulants and other drugs. *Lancet.* 1963; 2(7300): 175-176.
- [46] Zhang N, Czepielewski RS, Jarjour NN, Erlich EC, Esaulova E, Saunders BT, et al. Expression of factor V by resident macrophages boosts host defense in the peritoneal cavity. *J Exp Med.* 2019; 216(6): 1291-1300.
- [47] Lin X, Luo H, Yan X, Song Z, Gao X, Xia Y, et al. Interleukin-34 ameliorates survival and bacterial clearance in polymicrobial sepsis. *Crit Care Med.* 2018; 46(6): e584-e590.
- [48] Ito T, Shintani Y, Fields L, Shiraishi M, Podaru MN, Kainuma S, et al. Cell barrier function of resident peritoneal macrophages in post-operative adhesions. *Nat Commun.* 2021; 12(1): 2232.
- [49] Venet F, Cour M, Rimmelé T, Viel S, Yonis H, Coudereau R, et al. Longitudinal assessment of IFN- $\gamma$  activity and immune profile in critically ill COVID-19 patients with acute respiratory distress syndrome. *Crit Care.* 2021; 25(1): 140.
- [50] He W, Xiao K, Xu J, Guan W, Xie S, Wang K, et al. Recurrent sepsis exacerbates CD4<sup>+</sup> T cell exhaustion and decreases antiviral immune responses. *Front Immunol.* 2021; 12: 627435.
- [51] Wang G, Inturi S, Serkova NJ, Merkulov S, McCrae K, Russek SE, et al. High-relaxivity superparamagnetic iron oxide nanoworms with decreased immune recognition and long-circulating properties. *ACS Nano.* 2014; 8(12): 12437-49.
- [52] Sruthi S, Maurizi L, Nury T, Sallem F, Boudon J, Riedinger JM, et al. Cellular interactions of functionalized superparamagnetic iron oxide nanoparticles on oligodendrocytes without detrimental side effects: Cell death induction, oxidative stress and inflammation. *Colloids Surf B Biointerfaces.* 2018; 170: 454-462.
- [53] Liu XG, Zhang L, Lu S, Liu DQ, Huang YR, Zhu J, et al. Superparamagnetic iron oxide nanoparticles conjugated with  $\text{A}\beta$  oligomer-specific scFv antibody and class A scavenger receptor activator show therapeutic potentials for Alzheimer's Disease. *J Nanobiotechnology.* 2020; 18(1): 160.
- [54] Petzer V, Tymoszuk P, Asshoff M, Carvalho J, Papworth J, Deantonio C, et al. A fully human anti-BMP6 antibody reduces the need for erythropoietin in rodent models of the anemia of chronic disease. *Blood.* 2020; 136(9): 1080-1090.

- [55] Corradini E, Buzzetti E, Dongiovanni P, Scarlini S, Caleffi A, Pelusi S, et al. Ceruloplasmin gene variants are associated with hyperferritinemia and increased liver iron in patients with NAFLD. *J Hepatol.* 2021; 75(3): 506-513.
- [56] Tabbah SM, Buhimschi CS, Rodewald-Millen K, Pierson CR, Bhandari V, Samuels P, et al. Hepcidin, an iron regulatory hormone of innate immunity, is differentially expressed in premature fetuses with early-onset neonatal sepsis. *Am J Perinatol.* 2018; 35(9): 865-872.
- [57] Muriuki JM, Mentzer AJ, Band G, Gilchrist JJ, Carstensen T, Lule SA, et al. The ferroportin Q248H mutation protects from anemia, but not malaria or bacteremia. *Sci Adv.* 2019; 5(9): eaaw0109.
- [58] Mertens C, Mora J, Ören B, Grein S, Winslow S, Scholich K, et al. Macrophage-derived lipocalin-2 transports iron in the tumor microenvironment. *Oncoimmunology.* 2017; 7(3): e1408751.
- [59] Kang SS, Ren Y, Liu CC, Kurti A, Baker KE, Bu G, et al. Lipocalin-2 protects the brain during inflammatory conditions. *Mol Psychiatry.* 2018; 23(2): 344-350.
- [60] Chen PC, Shao YT, Hsieh MH, Kao HF, Kuo WS, Wang SM, et al. Early-life EV-A71 infection augments allergen-induced airway inflammation in asthma through trained macrophage immunity. *Cell Mol Immunol.* 2021; 18(2): 472-483.
- [61] Sun Z, Pan Y, Qu J, Xu Y, Dou H, Hou Y. 17 $\beta$ -estradiol promotes trained immunity in females against sepsis via regulating nucleus translocation of RelB. *Front Immunol.* 2020; 11: 1591.
- [62] van Vught LA, Klein Klouwenberg PM, Spitoni C, Scicluna BP, Wiewel MA, Horn J, et al. Incidence, risk factors, and attributable mortality of secondary infections in the Intensive Care Unit after admission for sepsis. *JAMA.* 2016; 315(14): 1469-79.
- [63] van Vught LA, Wiewel MA, Hoogendijk AJ, Frencken JF, Scicluna BP, Klein Klouwenberg PMC, et al. The host response in patients with sepsis developing Intensive Care Unit-acquired secondary infections. *Am J Respir Crit Care Med.* 2017; 196(4): 458-470.
- [64] Patoli D, Mignotte F, Deckert V, Dusuel A, Dumont A, Rieu A, et al. Inhibition of mitophagy drives macrophage activation and antibacterial defense during sepsis. *J Clin Invest.* 2020; 130(11): 5858-5874.
- [65] Carestia A, Mena HA, Olexen CM, Ortiz Wilczyński JM, Negrotto S, Errasti AE, et al. Platelets promote macrophage polarization toward pro-inflammatory phenotype and increase survival of septic mice. *Cell Rep.* 2019; 28(4): 896-908.e5.